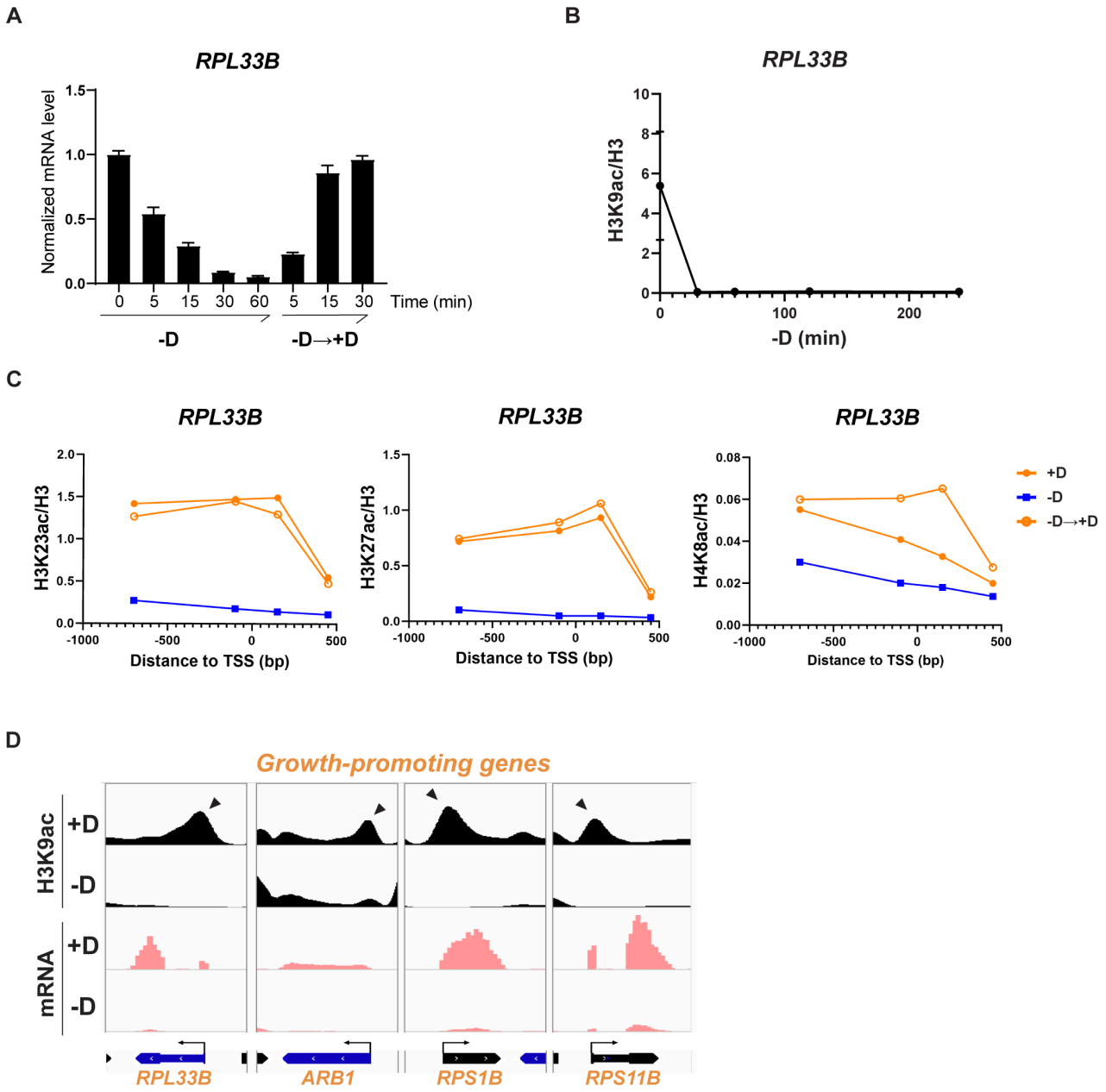

Figure S1, related to Figure 1. Acetylation sites on H3 at the promoter of ribosomal protein genes are responsive to glucose availability

(A) RT-PCR analysis of transcripts amounts of *RPL33B*, a representative ribosomal protein subunit gene, in response to changes in glucose availability.

(B) ChIP-PCR analysis of H3K9ac occupancy at *RPL33B* as a function of glucose starvation (-D) time: 0, 30, 60, 120, 240 min. All signals were normalized to H3.

(C) ChIP-PCR analysis of H3K23ac, H3K27ac and H4K8ac occupancy flanking TSS of *RPL33B*. Three conditions were assayed: glucose-replete (+D), glucose starvation for 30 min (-D), and glucose replenished for 30 min (-D→+D). All signals were normalized to H3.

(D) Genome browser view of ChIPseq data showing H3K9ac occupancy (in black) and mRNA levels (in pink) at representative growth-promoting genes under glucose-replete (+D) or glucose starvation (-D) conditions. Arrowheads indicate the peaks of H3K9ac that reside at the TSS of genes of interest.

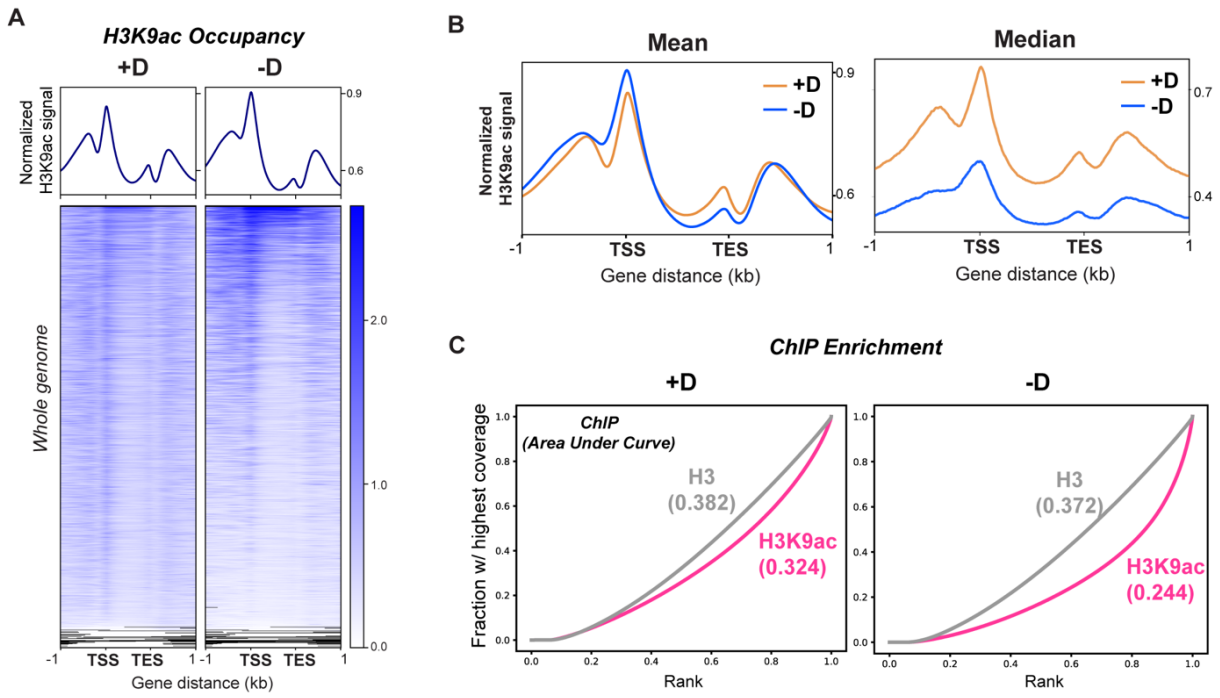

Figure S2, related to Figure 1. Genome-wide analysis of the refocusing of H3K9ac following glucose starvation

(A) ChIP-seq data showing genomic occupancy of H3K9ac under two conditions. Cells were collected from either glucose-replete (+D) or glucose starvation for 30 min (-D) for all ChIP-seq data performed in this study. Depicted genomic region spans 1 kb upstream of TSS (transcription start site) to 1 kb downstream of TES (transcription end site). Upper panel depicts the metagene profile in the mean of the signals. Lower panels present the heatmaps: genes shown in each row are the same between the two samples and sorted in descending order by signal intensity under glucose starvation condition.

(B) Metagene profile of H3K9ac ChIP-seq data showing either the mean or median of the signals across genes comparing glucose-replete (+D) or glucose starvation (-D) conditions. The region examined starts from 1 kb upstream of TSS to 1 kb downstream of TES. Note that while the mean signal was similar between the two conditions, the median signal was more prominent under glucose-replete conditions.

(C) Fingerprint plots depicting the profile of cumulative read coverages in each ChIP experiment comparing sample DNA versus input DNA. Grey lines denote the input DNA from H3 ChIP-seq; pink line denotes the sample DNA from H3K9ac ChIP-seq. The two graphs shown are one replicate of WT cells in either glucose-replete (+D) or glucose starvation (-D) conditions. Area under curve (AUC) suggests enrichment of ChIP samples: the lower the number, the more enriched the sample. H3K9ac signals were more enriched under glucose starvation than glucose-replete condition, while H3 enrichment remained consistent between the two conditions. Quantified data are shown in Figure S7A.

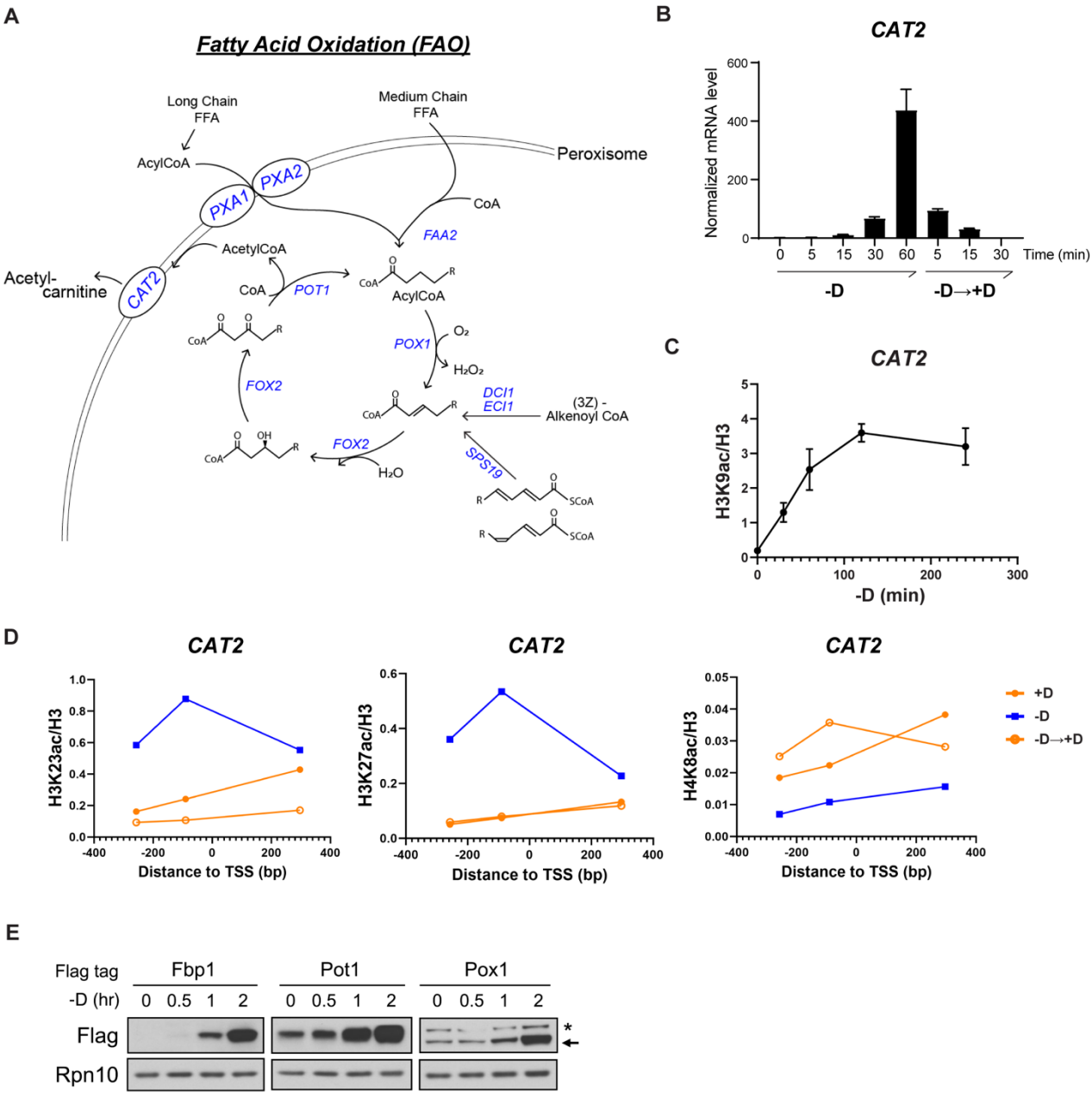

Figure S3, related to Figure 3. Gluconeogenic and fat metabolism genes are induced in an H3K9ac-dependent manner upon glucose starvation

(A) Key steps of (peroxisomal) fatty acid oxidation in budding yeast. Genes highlighted in blue are preferentially modified by H3K9ac in the set of starvation-induced genes.

(B) RT-PCR analysis of transcript amounts of *CAT2*, a representative fat metabolism gene, in response to changes in glucose availability. All signals were normalized to actin gene *ACT1*.

(C) ChIP-PCR analysis of H3K9ac occupancy at *CAT2* as a function of glucose starvation (-D) time: 0, 30, 60, 120, 240 min. All signals were normalized to H3.

(D) ChIP-PCR analysis of H3K23ac, H3K27ac and H4K8ac occupancy flanking TSS of *CAT2*. Three conditions were assayed: glucose-replete (+D), glucose starvation for 30 min (-D), and glucose replenished for 30 min (-D→+D). All signals were normalized to H3.

(E) Immunoblot was performed against Flag-tagged proteins in response to glucose availability. Fbp1p, Pot1p and Pox1p are enzymes encoded by candidate gluconeogenic and fat metabolism genes. Arrow indicates Pox1p; asterisk indicates a non-specific band.

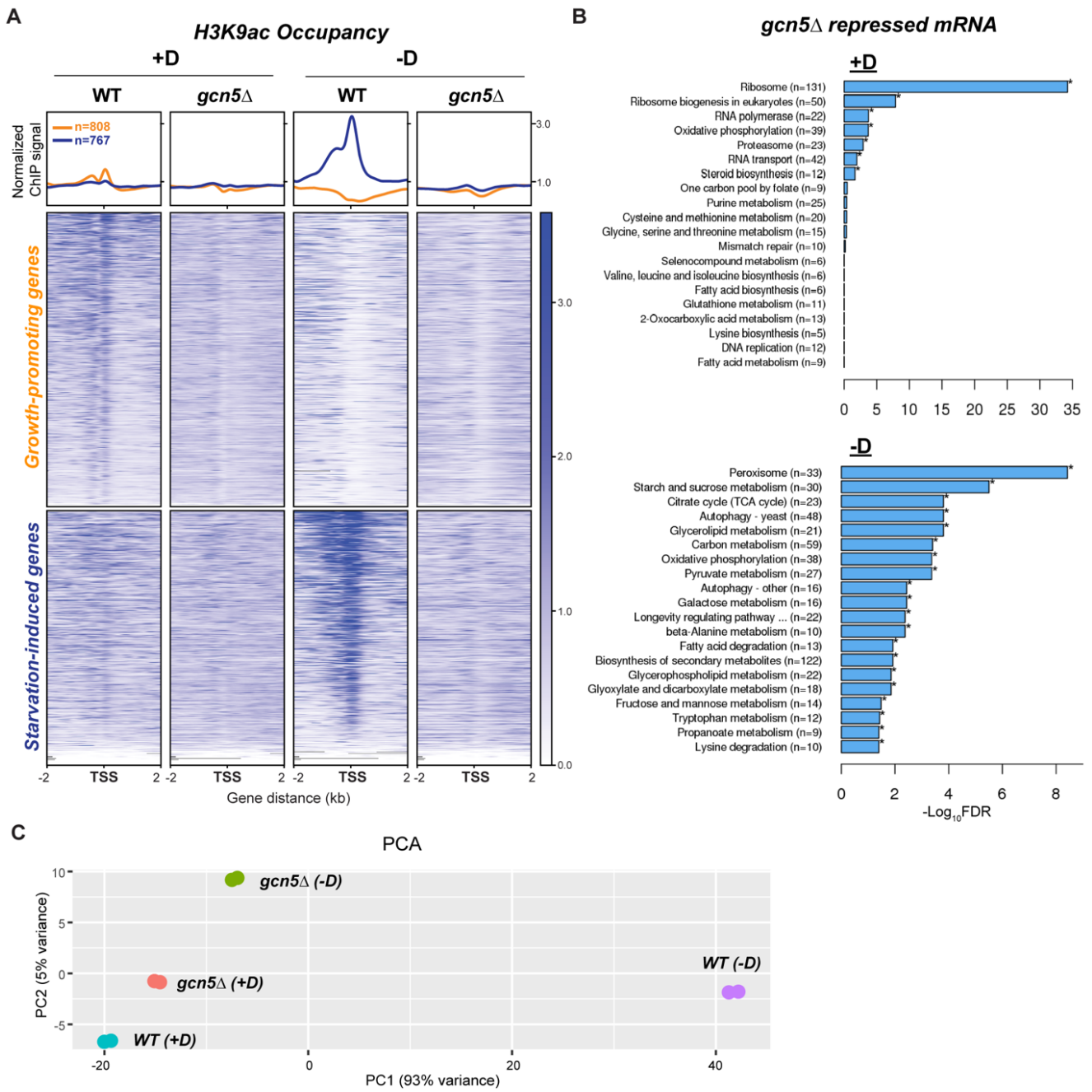

Figure S4, related to Figure 4. Gcn5p is required for proper transcriptional regulation in response to glucose availability

(A) ChIP-seq data displaying H3K9ac occupancy at two subsets of genes in WT and *gcn5Δ* cells in glucose-replete or glucose starvation conditions. Metagene profile plots the average signals from each subset of genes: growth-promoting genes in orange and starvation-induced genes in blue. Upper heatmaps consist of growth-promoting genes, ranked by signals in WT cells under glucose-replete condition; lower heatmaps consist of starvation-induced genes, ranked by signals in WT cells under glucose starvation. Genes shown in rows are the same among all four samples.

(B) Pathway enrichment analysis for transcripts that were repressed in *gcn5Δ* cells under glucose-replete (+D) or glucose starvation (-D) conditions.

(C) Principal component analysis (PCA) of RNA-seq data for WT and *gcn5Δ* cells. The variation exhibited in PC1 between the two conditions in WT cells was diminished in *gcn5Δ* cells.

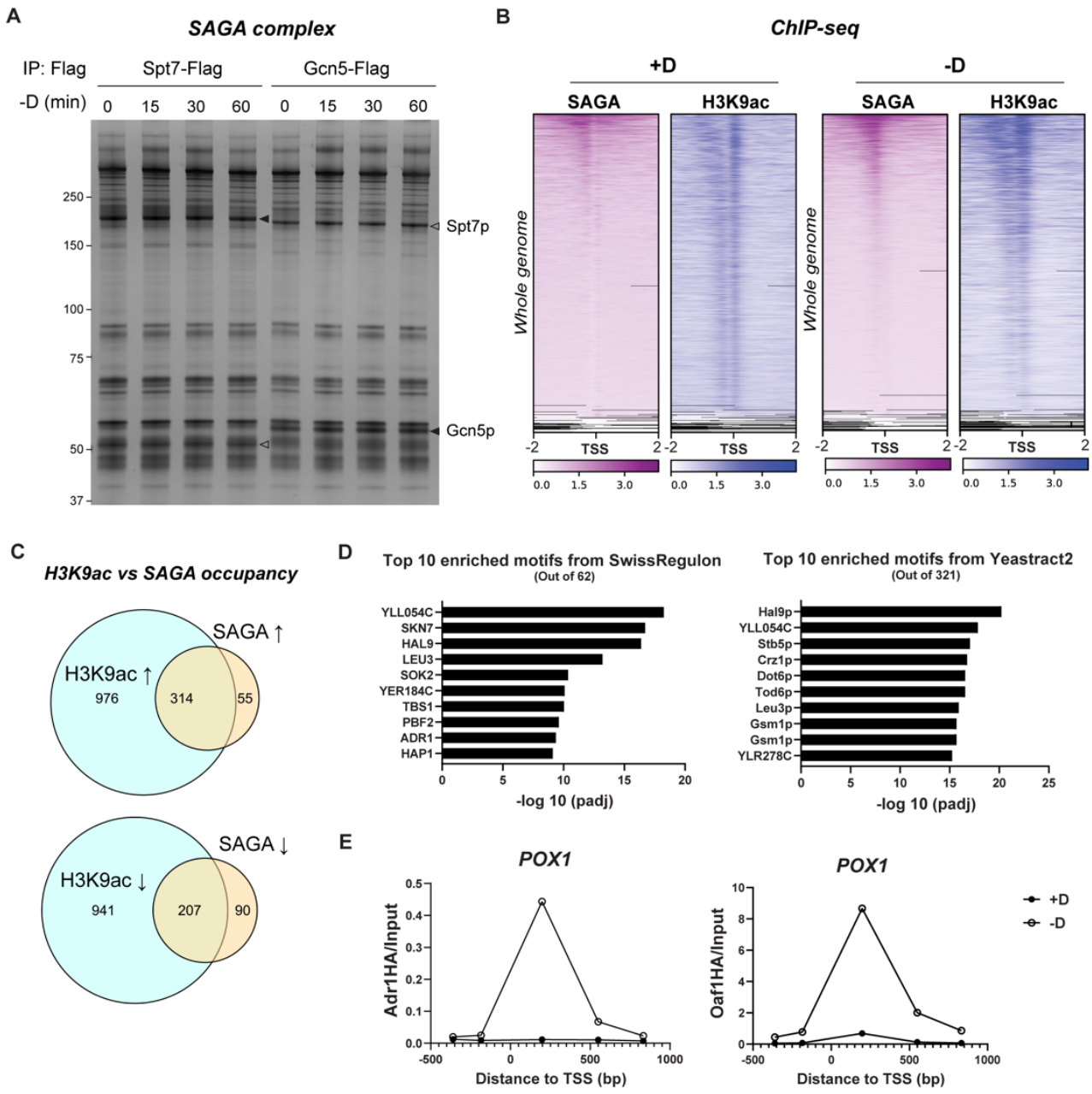

Figure S5, related to Figure 5. SAGA coordinates with starvation-specific transcription factors following glucose starvation

(A) Composition of the SAGA complex before and after glucose starvation. Immunoprecipitation was performed against Flag-tagged proteins, using either the scaffolding subunit Spt7p or Gcn5p. Empty arrowheads indicate untagged version of the indicated proteins. Solid arrowheads indicate Flag-tagged proteins.

(B) ChIP-seq data displaying the co-occupancy of SAGA and H3K9ac before and after glucose starvation. Genes were ranked in descending order by signal intensity from SAGA occupancy in each condition, respectively. Genes shown in rows are the same between the two ChIP-seq data sets.

(C) Venn diagrams from ChIP-seq data showing overlapping genes that were differentially modified by H3K9ac and bound by SAGA upon glucose starvation.

(D) Motif enrichment analysis for genes up-regulated in H3K9ac signal following glucose starvation. Note that in the Yeastract2 database, some transcription factors have more than one predicted motif, which may lead to multiple occurrences (e.g., Gsm1p). See also Table S2.

(E) ChIP-PCR analysis of Adr1p and Oaf1p occupancy flanking TSS of *POX1* under glucose-replete (+D) or glucose starvation (-D) conditions. All signals were normalized to input DNA.

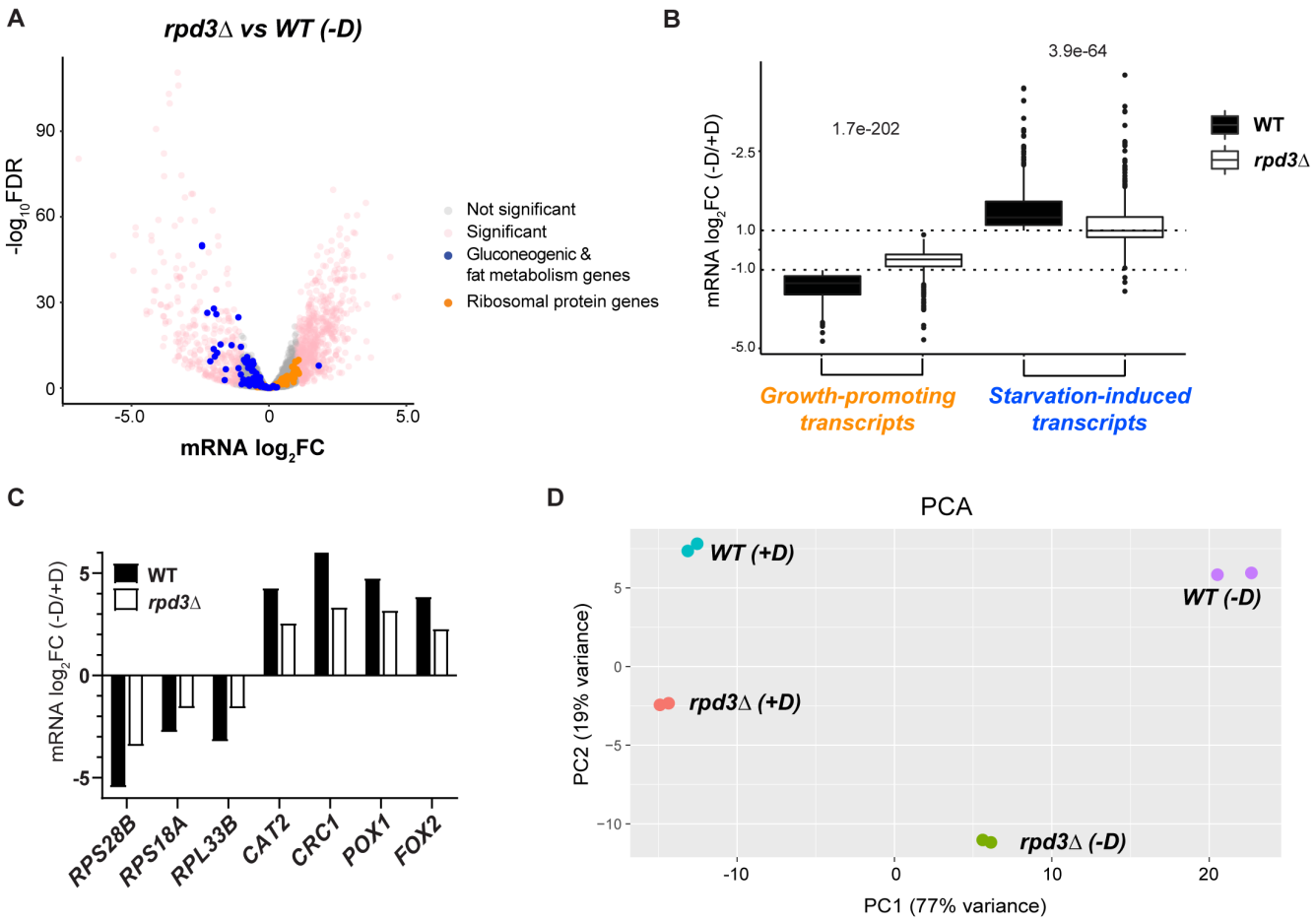

Figure S6, related to Figure 6. Rpd3p is required for proper transcriptional regulation in response to glucose availability

(A) Volcano plot of RNA-seq data showing differential gene expression in *rpd3Δ* cells compared to WT under glucose starvation condition (-D). Thresholds of 2-fold change (FC) and 0.05 FDR were considered as significant. Gluconeogenic and fat metabolism genes are colored in blue. Ribosomal protein genes are colored in orange.

(B) Box-whisker plot from RNA-seq data showing fold change in gene expression upon glucose starvation in WT and *rpd3Δ* cells. X-axis depicts two subsets of transcripts: growth-promoting or starvation-induced genes. Y-axis plots the $\log_2$ fold change of transcript amounts upon glucose starvation. P-values were determined by Kruskal-Wallis test.

(C) Differential expression from RNA-seq data displaying representative ribosomal protein genes (*RPS28B, RPS18A, RPL33B*) or fat metabolism genes (*CAT2, CRC1, POX1, FOX2*).

(D) Principal component analysis (PCA) of RNA-seq data for WT and *rpd3Δ* cells. The variation exhibited in PC1 between two conditions in WT cells was diminished in *rpd3Δ* cells.

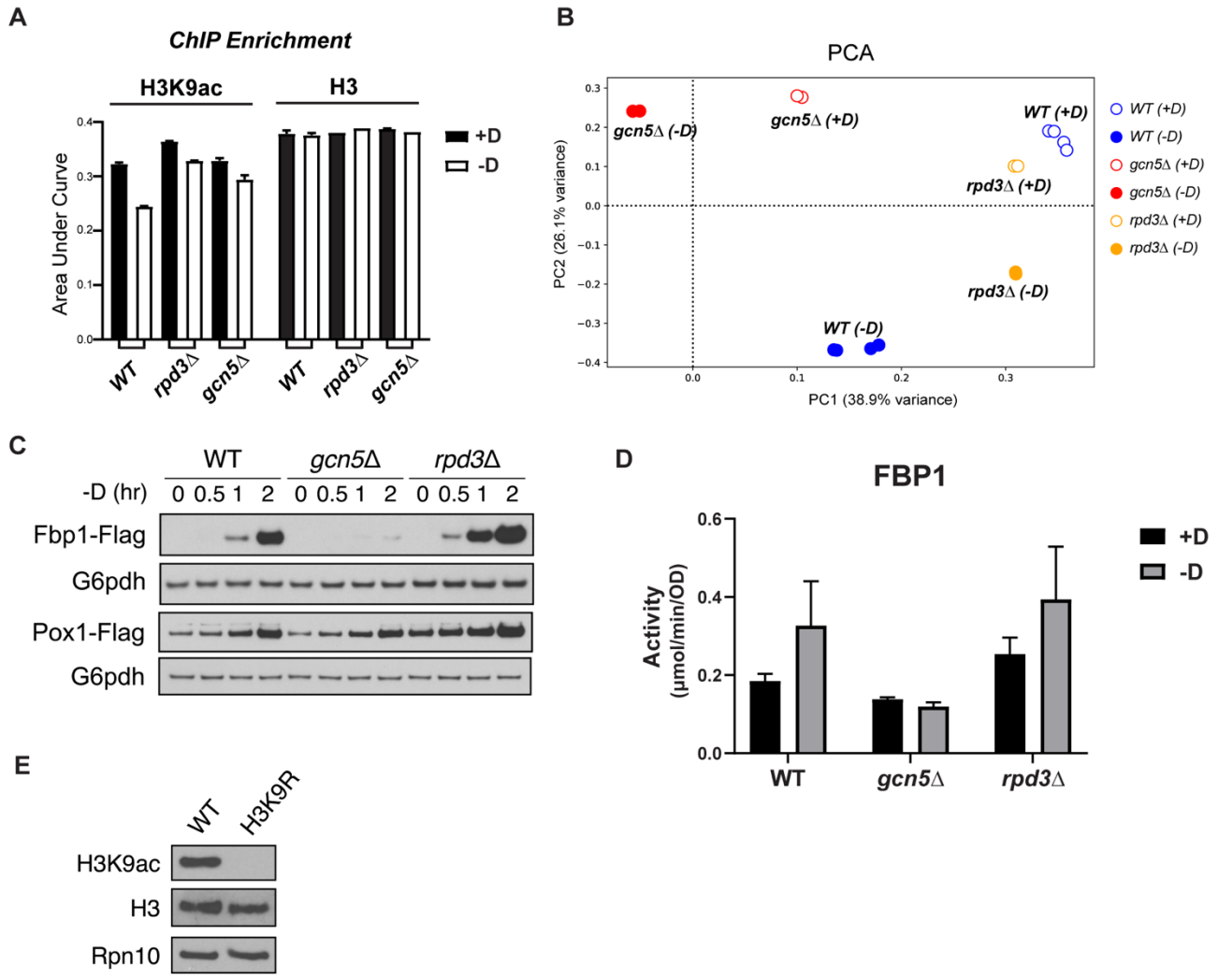

Figure S7, related to Figure 7. Gcn5p and Rpd3p are both required for proper epigenetic regulation to support cell growth upon glucose starvation

(A) Quantification of area under curve (AUC) from fingerprint plots enrichment analysis. Glucose-replete conditions (+D) are depicted in black bars; glucose starvation conditions (-D) in white bars. Strain genotypes of the ChIP samples are as denoted at the bottom. Note the significant difference between glucose-replete and glucose starvation conditions for WT cells. This difference was diminished in both gcn5Δ and rpd3Δ cells. In addition, both *gcn5*Δ and *rpd3*Δ cells showed less enrichment in glucose starvation conditions compared to WT cells.

(B) Principal component analysis (PCA) of all samples from H3K9ac ChIP-seq. Glucose-replete conditions (+D) are shown in empty circles; glucose starvation conditions (-D) are shown in solid circles. Strain genotypes are denoted in different colors.

(C) Immunoblot was performed against the indicated Flag-tagged proteins in response to glucose availability. Fbp1p and Pox1p are encoded by candidate gluconeogenic and fat metabolism genes.

(D) Fructose-1,6-bisphosphatase (Fbp) activity assay was performed using a commercially available kit. Cells were collected from glucose-replete (+D) or glucose starvation conditions for 2 hr (-D). Activity was quantified by subtracting signals at two time points within linear range.

(E) Specificity of H3K9ac antibody. Note that cells expressing histone H3 genes with a K9 -> R point mutation grown to log phase exhibited no detectable signal from the H3K9ac antibody utilized in this study.

Table S3, related to STAR Methods. Primers used in this study

ACT1_RT_F	RT-qPCR	TCCGGTGATGGTGTTACTCA
ACT1_RT_R	RT-qPCR	GGCCAAATCGATTCTCAAAA
POX1_RT_F	RT-qPCR	TGAGACAGACTTGCGGAGGA
POX1_RT_R	RT-qPCR	CTGAACCACCCAGTCGTCAT
CAT2_RT_F	RT-qPCR	GGCGGAAAAGCCGAACAAAT
CAT2_RT_R	RT-qPCR	TTCGGGCACGGGTAATGATG
RPL33B_RT_F	RT-qPCR	GGGGCAAAGTCACCAGAACTCACG
RPL33B_RT_R	RT-qPCR	GCACCGAAAGTCTTGGCTGGCA
CAT2_F1	ChIP-qPCR	TCCTCTCAAAGTCATCCTTGTTC
CAT2_R1	ChIP-qPCR	CCGGCGTTTAGTTGCTCTTA
CAT2_F2	ChIP-qPCR	GCACTCATGAGGATCTGTCATTC
CAT2_R2	ChIP-qPCR	GCATTGCTCTCCTTGACGTTAT
CAT2_F3	ChIP-qPCR	GATTGAAAGAGTATGCCAACGATAA
CAT2_R3	ChIP-qPCR	AGACGTATGGAACAATAGGATCG
RPL33B_F1	ChIP-qPCR	ACATACTGAAGTACGTCGACACAGATT
RPL33B_R1	ChIP-qPCR	TCCCCCACCAGACATATATAAAGG
RPL33B_F2	ChIP-qPCR	GTTTGTGCTGGCCTCTCCAT
RPL33B_R2	ChIP-qPCR	AGCAAGAACCCTTCACATGTCA
RPL33B_F3	ChIP-qPCR	GCCGTGGAATAGGCTGATTC
RPL33B_R3	ChIP-qPCR	GGCCCCAACTATAACACATGTTTT
RPL33B_F4	ChIP-qPCR	AGCACTTATCCTACCAAAGATCTAAGAGA
RPL33B_R4	ChIP-qPCR	GGCAACACCTTCAATCTTAATCAA